Light Funneling Mechanism Explained by Magnetoelectric Interference

Fabrice Pardo,[1,*] Patrick Bouchon,[1,2] Riad Haïdar,[2,3] and Jean-Luc Pelouard[1]

[1]*CNRS – Laboratoire de Photonique et de Nanostructures, Route de Nozay, 91460 Marcoussis, France*
[2]*Office National d'Études et de Recherches Aérospatiales, Chemin de la Hunière, 91761 Palaiseau, France*
[3]*École Polytechnique, Département de Physique, 91128 Palaiseau, France*

(Received 26 October 2010; revised manuscript received 8 June 2011; published 24 August 2011)

We investigate the mechanisms involved in the funneling of optical energy into subwavelength grooves etched on a metallic surface. The key phenomenon is unveiled thanks to the decomposition of the electromagnetic field into its propagative and evanescent parts. We unambiguously show that the funneling is not due to plasmonic waves flowing toward the grooves, but rather to the magnetoelectric interference of the incident wave with the evanescent field, this field being mainly due to the resonant wave escaping from the groove.

DOI: 10.1103/PhysRevLett.107.093902 PACS numbers: 42.82.Et, 42.25.Fx, 42.79.Ag, 78.67.−n

Plasmonics, as the science of the efficient coupling of photons with free electron gas oscillation modes at the surface of metals, appears as an inescapable solution for the design and realization of optical nanoantennas [1]. Numerous cutting edge applications are based on nanoantennas like biosensing [2], gas sensing [3], photovoltaic [4] or infrared photodetection [5], which exploit the intense local electromagnetic field in a confined volume [6–8]. Now, the specific matter of total photon harvesting at the nanometric scale, i.e., designing an antenna able to couple all the incident optical power with a nanoabsorber, remains challenging [1,7–9]. The natural two-step antenna sequence (collection of light, then concentration) has been extensively studied in structures made of a metallic subwavelength grating surrounding a target [6,10–14]. The underlying mechanism involves surface plasmon polariton (SPP) excitation (collection) and propagation (concentration) along the grating toward the target. Such structures, though, are designed to collect light at a specific incidence angle, which is obviously a strong practical limitation.

In contrast, quasi-isotropic perfect transmission is obtained through very narrow slits drilled in a metallic membrane [15,16]. This perfect transmission is successfully explained by a localized Fabry-Perot resonance in the slits [17]. However the funneling, namely, the mechanism responsible for the redirection and subsequent concentration of the whole incident energy flow, from the surface toward the tiny aperture of the slits, remains unclear. Yet, a pictorial model of the underlying physics is of key importance for the design of efficient nanoantennas.

Such a model is given by the energetic point of view [18]: Poynting-vector streamlines distinctly show that the incident flow bends when reaching the metal surface, and then propagates along the interface toward the slits. This fits with the intuitive explanation, inspired by the SPP excitation process, that plasmonic waves drive the funneling sequence [19]. Furthermore, quasicylindric waves were recently identified as the dominant short-range propagation process of the field amplitude along the surface of the grating [20,21]. Nevertheless, even if the evanescent waves are naturally assumed to concentrate the energy toward the apertures of the slits, no specific study of the light funneling has so far been carried out to our knowledge.

In this Letter, we definitely unveil the funneling process, and highlight the unexpectedly limited role of the evanescent waves alone. First, by analyzing the particular case of a groove (for which experimental study confirm theoretical predictions [22]), we show that the evanescent waves do not carry any energy through the apertures: they simply redistribute it over the metal surface. Instead, we identify the magnetoelectric interference (MEI) [23] of the incident wave with the evanescent field as the main mechanism of the funneling sequence. We then use a single interface analysis [24] to generalize our result to subwavelength apertures with no resonator behind. MEI also explains the broadband extraordinary transmission due to plasmonic Brewster angle that was recently published by Alù [25] (see Supplemental Material [22]).

Let us consider an infrared light at $\lambda_f = 4\ \mu$m incident onto nanometric sized grooves periodically drilled into a gold surface. Figure 1(a) shows the geometry of the grating (width $w = 56$ nm, height $h = 640$ nm and period d). The period is chosen so that there is no diffracted wave for all angles of incidence (hence $d \leq \lambda_f/2$). The light is TM polarized (transverse magnetic) and incident with an angle θ. The dielectric function of gold is computed from the Drude model $\varepsilon(\lambda) = 1 - [(\lambda_p/\lambda + i\gamma)\lambda_p/\lambda]^{-1}$ which is suited to the infrared spectral range for $\lambda_p = 161$ nm and $\gamma = 0.0077$ [26]. The electromagnetic analysis of this structure is done using a B-spline method [27], which can perform fast and exact computation of Maxwell equations. The Poynting-vector streamlines show how the energy flow is funneled toward the apertures, and dissipated mainly on the sidewalls of the grooves. The reflectivity of the grating is plotted in Fig. 1(c) at normal incidence for $d = \lambda_f/2$ and for a random value $d = 1.618\ \mu$m.

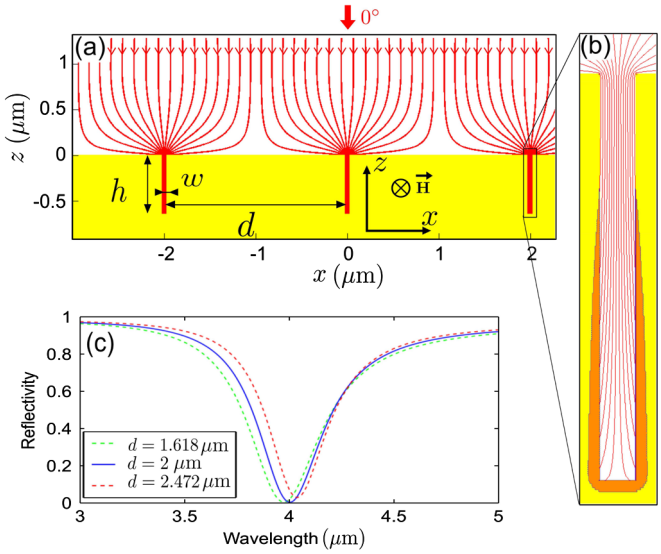

FIG. 1 (color online). (a) Poynting-vector streamlines are drawn on a grating of grooves of height $h = 640$ nm, width $w = 56$ nm and period $d = 2$ μm. The incident energy is funneled inside the grooves. (b) Vector streamlines inside a groove. The dissipation of the energy is computed in the metallic region, it clearly appears that this dissipation occurs on the sidewalls of the grooves (orange [dark gray] volume), see [22] for detailed field maps. (c) Reflectivity spectra for various values of the grating period $d = 1.618$ μm, $d = 2$ μm, and $d = 2.472$ μm. The geometry of the groove is the same as before. The period has almost no influence on the resonance since it is due to the Fabry-Perot resonator inside the grooves.

Although the grating is structured on a tiny portion of its surface (less than 3%), it exhibits a resonance with a total absorption at normal incidence. We should highlight that λ_f depends only slightly on the period d. Additionally quasi total absorption is predicted even for large incidence angles ($\theta \leq 50°$), which is adapted to light collecting systems.

In order to address the funneling mechanism, we consider the electromagnetic field in the air, and we split it into three terms. The magnetic field is expressed:

$$H_{\text{total}} = H_i + H_r + H_e, \tag{1}$$

where H_i is the incoming wave, H_r is the reflected wave, and H_e is the sum of the diffracted evanescent waves. Similar definitions can be given for the electric field components. In the rest of this Letter, $E \times H$ stands for the mean time average value of the vectorial product and is practically computed from complex amplitudes as $\frac{1}{2}\text{Re}(E \times H^*)$. Thanks to the decomposition of Eq. (1), the Poynting vector can be expressed as the sum of six terms:

$$S = S_i + S_{ei} + S_r + S_{er} + S_e + S_{ir}, \tag{2}$$

with $S_i = E_i \times H_i$, $S_{ei} = E_e \times H_i + E_i \times H_e$, $S_r = E_r \times H_r$, $S_{er} = E_e \times H_r + E_r \times H_e$, $S_e = E_e \times H_e$, and $S_{ir} = E_i \times H_r + E_r \times H_i$. The terms S_i and S_r are, respectively, the incident and the reflected fluxes of the plane wave. The term S_e corresponds to the energy carried by the evanescent waves. The term S_{ei} corresponds to the MEI between the evanescent and the incident fields. It is easy to prove that the six terms of Eq. (2) are flux conservative (null divergence) thus each of them can be considered to be an independent energy flux vector in the air. In order to simplify the discussion, we first consider an optimized device at the resonance wavelength. So no wave is reflected, the fields H_r and E_r are null and the Poynting-vector can be expressed as $S = S_i + S_{ei} + S_e$.

The Poynting-vector streamlines for S_i, S_{ei} and S are plotted at two angles of incidence in Fig. 2 so that the flux of energy between two lines is constant.

At normal incidence, as expected for a propagative plane wave in air, the lines for incident flux S_i are equidistant and in the propagation direction. The MEI S_{ei} lines are coming from the surface and are converging on the groove. On the metallic surface, they compensate for the flux of the incident plane wave and funnel it inside the groove. By drawing lines perpendicular to the Poynting streamlines on Fig. 2(c), and taking into account that the predominant term in S_{ei} is $E_e \times H_i$, one can deduce that the evanescent wave shape is quasicylindrical [20,21]. The evanescent flux S_e (not shown) carries energy 1000 times weaker and does not play an active role in the funneling for this structure at normal incidence. In Fig. 2(e), the total flux of energy S is shown to funnel into the groove in the near-field region ($z \lesssim 500$ nm). Eventually all the incident flux is dissipated, mostly inside the groove.

For an incidence of 30°, the MEI S_{ei} is still funneling the energy towards the slits [Fig. 2(d)]. However, we can notice there are more lines going out from the metal surface on the left (10 lines) than on the right (6 lines). Nonetheless, Fig. 2(f) shows that the incident energy gets funneled into the groove despite this asymmetry. In fact, at oblique incidence, the evanescent field carries an energy flux S_e which is no longer negligible, as shown in Fig. 3: the energy is redirected from the right side of the groove to the left side. This redistribution of the energy compensates for the dissymmetry of S_{ei} which appears in Fig. 2(d). In conclusion S_e plays no role in the funneling, but helps to redistribute energy over the grating. This incidentally invalidates the hypothetical role of plasmonic waves, which are evanescent waves, in the funneling mechanism. As a general comment, it is interesting to point out that the MEI process is known to be responsible for the optical tunnelling (frustrated total reflection) [28]. Our study unveils its key role in a larger spectrum of near-field energy transfer phenomena.

We now aim to describe the origin of the evanescent field involved in the funneling process. The subwavelength groove behaves as a Fabry-Perot resonator. As in Ref. [24], we consider the isolated single interface in two configurations: one where the incident field is a unit-amplitude plane wave in air; the other where the incident field is a wave coming from the bottom of the groove, and is unit-amplitude at the interface. In the first case [Fig. 4(a)] the reflected wave has an amplitude ρ_1 and an evanescent field η_1. Because of the low aperture ratio w/d, we get $|\rho_1| \lesssim 1$

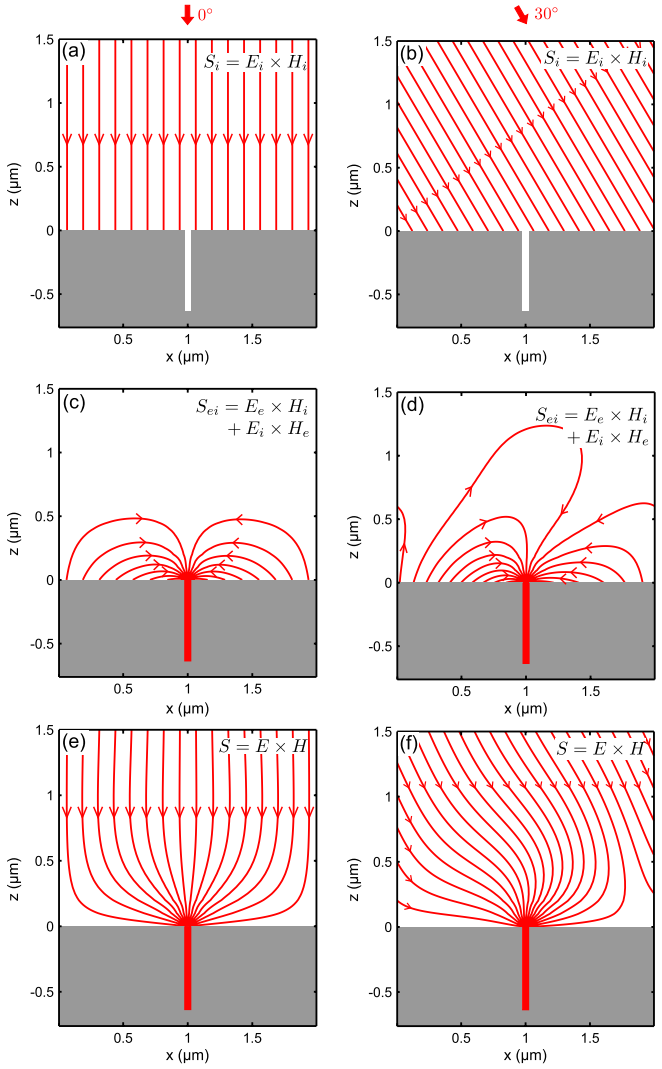

FIG. 2 (color online). Poynting-vector streamlines in one period of the slit grating for two angles of incidence $\theta = 0°$ (left column) and $\theta = 30°$ (right column) at $\lambda = 4000$ nm. Streamlines of the incident wave are shown in (a) and (b). Streamlines of the interference between the incident wave and the evanescent field are shown in (c) and (d). The energy flux of the evanescent waves is negligible in this structure for $\theta = 0°$; refer to Fig. 3(a) for an illustration at $\theta = 30°$. Streamlines of the total Poynting vector are shown in (e) and (f). In both cases, the incident energy is funneled inside the groove where it is fully absorbed inside the metal.

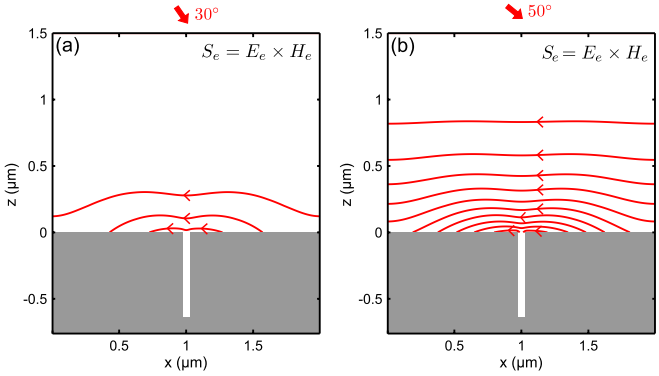

FIG. 3 (color online). Poynting-vector streamlines of the evanescent field for two angles of incidence (a) 30° and (b) 50° at $\lambda = 4000$ nm. S_e does not play a role in funneling but redistributes the energy in the grating.

and $|\eta_1| \ll 1$. In the second case [Fig. 4(b)] the transmitted wave (which corresponds to the reflected wave above) has an amplitude τ_2 and the evanescent field in the air is written η_2. If a unit-amplitude wave is defined as taking the value $H_y = 1$ at the center of a groove entrance, then computation shows that evanescent amplitudes η_1 and η_2 are nearly equal. Because of the low aperture ratio w/d, we get $|\tau_2| \ll 1$.

At the resonance, the wave coming from the bottom of the groove has an amplitude $A = -\tau_2^{-1}\rho_1$ so that all the amplitudes in Fig. 4(b) are multiplied by the factor A, which leads to Fig. 4(c). The response of the grating excited by a unit-amplitude plane wave at this resonance is thus given by the superposition of the amplitudes of Figs. 4(a) and 4(c), shown on Fig. 4(d). This leads to the expected null-amplitude reflected wave. Moreover, the resulting evanescent field is expressed as $\eta_1 + \eta_2 A \simeq \eta_2 A$ because $|\eta_1| \simeq |\eta_2|$ and $A \gg 1$ (e.g., for the grating described in Fig. 1, one computes $|A| \simeq 11$). To summarize, the wave built inside the grooves escapes in the air as both a propagating plane wave $\tau_2 A$ and an evanescent field $\eta_2 A$ [see Fig. 4(c)]. The propagating plane wave interferes destructively with the directly reflected wave ($\tau_2 A + \rho_1 = 0$) leading to the null reflection, and the evanescent field interferes with the incoming plane wave to funnel the energy into the groove. The two effects are of course not independent: we have no reflection because the energy is nearly fully collected in the groove. As a generalization path, it is interesting to note that this analysis still holds whatever the structure etched behind the aperture on the metal surface (rectangular slits, or more complex shapes such as in Ref. [29]).

Finally, we want to highlight that the key role played by the MEI of propagative waves with the evanescent field in the funneling mechanism is not limited to resonant structures. Let us thus consider the nonresonant case of a grating made of infinitely deep grooves, i.e., the simple isolated interface illustrated in Fig. 4(a), with a reflected wave of amplitude ρ_1. For an incidence angle of 30°, we get $|\rho_1|^2 = 0.83$: about 17% of the incident energy enters the grooves. This value is much larger than the aperture ratio $w/d = 2.8\%$, thus there appears to be funneling. Now, if we compare this to the situation of Fig. 4(d), the evanescent field of Fig. 4(a) is lowered by a factor $|\eta_1 + \eta_2 A|/|\eta_1| \simeq |A| \simeq 11$. We therefore compute that the interference of the incident wave with the evanescent field gives a funneling of about $1/|A| \simeq 9\%$. The missing 8% stems from the interference of the evanescent field with the reflected wave ρ_1, which paradoxically contributes to the funneling of energy inside the grooves. The key to the paradox lies here: first, the main contribution to the interference is $E_e \times H_r$

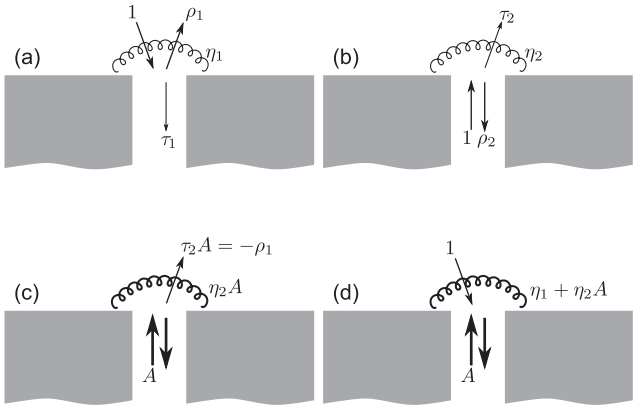

FIG. 4. Isolated single interface analysis of the metallic grating optimized to absorb all the incident light. (a) Unit plane wave from air: ρ_1 is the amplitude of the reflected plane wave, η_1 is the vector of evanescent field amplitudes. (b) Unit modal wave from bottom of grooves: τ_2 is the amplitude of the plane wave escaping in the air, η_2 is the vector of evanescent field amplitudes. (c) Same as (b), but with the modal wave having the amplitude A. (d) Superposition of (a) and (c), showing the field amplitudes in the grating excited by a unit plane wave: the reflectivity is null and the evanescent field is dominated by the term escaping from the resonator.

($E_r \times H_e$ is much smaller, at least at the interface level) and, second, the magnetic field H_r has the sign of H_i due to the metallic reflection.

In conclusion, we have unveiled the funneling mechanism of incident light in very narrow grooves etched on a metal surface. It originates from the magnetoelectric interference between the incident wave and the evanescent field, in both resonant and nonresonant situations. Furthermore, this result has been generalized to any subwavelength aperture etched on a metal surface (whatever the structure behind it) thanks to a single interface analysis. In the resonant case, the evanescent field escaping from the apertures can lead to the full harvesting of incident photons for a broad range of incidences. From a practical point of view, this approach opens a new avenue for the design of electromagnetic resonant antennas, based on the tailoring of the escaping evanescent field.

We have shown that evanescent waves propagating along the interface do not carry any energy through the apertures. This clearly demonstrates that the funneling is not mediated by plasmon waves at the surface.

This work was partially supported by the ANTARES Carnot project.

*fabrice.pardo@lpn.cnrs.fr

[1] P. Mühlschlegel, H. Eisler, O. Martin, B. Hecht, and D. Pohl, Science **308**, 1607 (2005).
[2] A. Kabashin, P. Evans, S. Pastkovsky, W. Hendren, G. Wurtz, R. Atkinson, R. Pollard, V. Podolskiy, and A. Zayats, Nature Mater. **8**, 867 (2009).
[3] N. Liu, M. Tang, M. Hentschel, H. Giessen, and A. Alivisatos, Nature Mater. **10**, 631 (2011).
[4] H. Atwater and A. Polman, Nature Mater. **9**, 205 (2010).
[5] M. Knight, H. Sobhani, P. Nordlander, and N. Halas, Science **332**, 702 (2011).
[6] S. Kim, J. Jin, Y.-J. Kim, I.-Y. Park, Y. Kim, and S.-W. Kim, Nature (London) **453**, 757 (2008).
[7] J. A. Schuller, E. S. Barnard, W. Cai, Y. C. Jun, J. S. White, and M. L. Brongersma, Nature Mater. **9**, 193 (2010).
[8] L. Novotny, Phys. Rev. Lett. **98**, 266802 (2007).
[9] L. Tang, S. E. Kocabas, S. Latif, A. K. Okyay, D.-S. LyGagnon, K. C. Saraswat, and D. A. B. Miller, Nat. Photon. **2**, 226 (2008).
[10] T. Thio, K. M. Pellerin, R. A. Linke, H. J. Lezec, and T. W. Ebbesen, Opt. Lett. **26**, 1972 (2001).
[11] T. Ishi, J. Fujikata, K. Makita, T. Baba, and K. Ohashi, Jpn. J. Appl. Phys. **44**, L364 (2005).
[12] Z. Yu, G. Veronis, S. Fan, and M. L. Brongersma, Appl. Phys. Lett. **89**, 151116 (2006).
[13] E. Laux, C. Genet, T. Skauli, and T. W. Ebbesen, Nat. Photon. **2**, 161 (2008).
[14] C. Genet and T. W. Ebbesen, Nature (London) **445**, 39 (2007).
[15] J. A. Porto, F. J. García-Vidal, and J. B. Pendry, Phys. Rev. Lett. **83**, 2845 (1999).
[16] S. Collin, F. Pardo, R. Teissier, and J.-L. Pelouard, Phys. Rev. B **63**, 033107 (2001).
[17] P. Lalanne, J. P. Hugonin, S. Astilean, M. Palamaru, and K. D. Möller, J. Opt. A **2**, 48 (2000).
[18] H. T. Miyazaki and Y. Kurokawa, IEEE J. Sel. Top. Quantum Electron. **14**, 1565 (2008).
[19] P. N. Stavrinou and L. Solymar, Opt. Commun. **206**, 217 (2002).
[20] H. Liu and P. Lalanne, Nature (London) **452**, 728 (2008).
[21] X. Y. Yang, H. T. Liu, and P. Lalanne, Phys. Rev. Lett. **102**, 153903 (2009).
[22] See Supplemental Material at http://link.aps.org/supplemental/10.1103/PhysRevLett.107.093902 for MEI interpretation of the plasmonic Brewster effect, experimental results, field maps, and scaling issues.
[23] In order to prevent any ambiguity with the traditional interference concept, namely $E_1 \cdot E_2$, we call the term $E_1 \times H_2 + E_2 \times H_1$ the magnetoelectric interference (MEI) of two waves 1 and 2.
[24] P. Lalanne, C. Sauvan, J. P. Hugonin, J. C. Rodier, and P. Chavel, Phys. Rev. B **68**, 125404 (2003).
[25] A. Alù, G. D'Aguanno, N. Mattiucci, and M. J. Bloemer, Phys. Rev. Lett. **106**, 123902 (2011).
[26] E. Palik, *Handbook of Optical Constants of Solids, Part II* (Academic Press, New York, 1985).
[27] P. Bouchon, F. Pardo, R. Haïdar, and J.-L. Pelouard, J. Opt. Soc. Am. A **27**, 696 (2010).
[28] G. S. Smith, *An Introduction to Classical Electromagnetic Radiation* (Cambridge University Press, Cambridge, England, 1997) ISBN 0521580935.
[29] T. V. Teperik, F. J. Garcia de Abajo, A. G. Borisov, M. Abdelsalam, P. N. Bartlett, Y. Sugawara, and J. J. Baumberg, Nat. Photon. **2**, 299 (2008).